

2  
ANL-AFP-30

MASTER

ANL-AFP-30

**THE BREEDING PERFORMANCE  
OF CARBIDE AND NITRIDE FUELS  
IN 2000 MWe LMFBRs**

**- A Preliminary Report -**

**Part I: Assumptions, Constraints and Methodology**

**by**

**W. P. Barthold**

**Applied Physics Division**



U of C - AUA - USERDA

---

**ARGONNE NATIONAL LABORATORY, ARGONNE, ILLINOIS**

**Prepared for the U. S. ENERGY RESEARCH**

**AND DEVELOPMENT ADMINISTRATION**

**under Contract W-31-109-Eng-38**

**DISTRIBUTION OF THIS DOCUMENT IS UNLIMITED**

---

## DISCLAIMER

**This report was prepared as an account of work sponsored by an agency of the United States Government. Neither the United States Government nor any agency Thereof, nor any of their employees, makes any warranty, express or implied, or assumes any legal liability or responsibility for the accuracy, completeness, or usefulness of any information, apparatus, product, or process disclosed, or represents that its use would not infringe privately owned rights. Reference herein to any specific commercial product, process, or service by trade name, trademark, manufacturer, or otherwise does not necessarily constitute or imply its endorsement, recommendation, or favoring by the United States Government or any agency thereof. The views and opinions of authors expressed herein do not necessarily state or reflect those of the United States Government or any agency thereof.**

## **DISCLAIMER**

**Portions of this document may be illegible in electronic image products. Images are produced from the best available original document.**

The facilities of Argonne National Laboratory are owned by the United States Government. Under the terms of a contract (W-31-109-Eng-38) between the U. S. Energy Research and Development Administration, Argonne Universities Association and The University of Chicago, the University employs the staff and operates the Laboratory in accordance with policies and programs formulated, approved and reviewed by the Association.

#### MEMBERS OF ARGONNE UNIVERSITIES ASSOCIATION

The University of Arizona	Kansas State University	The Ohio State University
Carnegie-Mellon University	The University of Kansas	Ohio University
Case Western Reserve University	Loyola University	The Pennsylvania State University
The University of Chicago	Marquette University	Purdue University
University of Cincinnati	Michigan State University	Saint Louis University
Illinois Institute of Technology	The University of Michigan	Southern Illinois University
University of Illinois	University of Minnesota	The University of Texas at Austin
Indiana University	University of Missouri	Washington University
Iowa State University	Northwestern University	Wayne State University
The University of Iowa	University of Notre Dame	The University of Wisconsin

#### NOTICE

This report was prepared as an account of work sponsored by the United States Government. Neither the United States nor the United States Energy Research and Development Administration, nor any of their employees, nor any of their contractors, subcontractors, or their employees, makes any warranty, express or implied, or assumes any legal liability or responsibility for the accuracy, completeness or usefulness of any information, apparatus, product or process disclosed, or represents that its use would not infringe privately-owned rights. Mention of commercial products, their manufacturers, or their suppliers in this publication does not imply or connote approval or disapproval of the product by Argonne National Laboratory or the U. S. Energy Research and Development Administration.

The Breeding Performance of Carbide and Nitride Fuels

in 2000 MWe LMFBRs

- A Preliminary Report -

Part I: Assumptions, Constraints and Methodology

W. P. Barthold

*Applied Physics Division*

NOTICE

This report was prepared as an account of work sponsored by the United States Government. Neither the United States nor the United States Energy Research and Development Administration, nor any of their employees, nor any of their contractors, subcontractors, or their employees, makes any warranty, express or implied, or assumes any legal liability or responsibility for the accuracy, completeness or usefulness of any information, apparatus, product or process disclosed, or represents that its use would not infringe privately owned rights.

September 1976

## List of Contents

	<u>Page</u>
Abstract	
I. Introduction	1
II. Scope and Limitations	2
III. Assumptions and Constraints	4
A) Assumptions	4
B) Constraints	12
a) Geometry Constraints	18
b) Performance Constraints	19
c) Constraints Coming from Fabrication Consideration	21
d) Operational Constraints	21
e) Fuel Bundle-Duct Interaction Constraints	22
IV. Methodology for Design and Analysis	23
V. Summary	33
Appendix A - The Definition of the Compound System Doubling Time	35
Appendix B - A Figure of Merit for Ore Conservation	39
Appendix C - Calculation of Interassembly Gaps (Duct Dilation)	42
References	47

## List of Tables

<u>No.</u>		<u>Page</u>
1.	Nuclear Design Assumptions	5
2.	Thermal Design Assumptions	8
3.	Mechanical Design Assumptions	9
4.	Material Behavior and Properties	13
5.	Basic Computational Flow for System Design Studies	24
C.1.	Nomenclature	46

## ABSTRACT

The assumptions, constraints and methodology used in the design and analysis of 2000 MWe LMFBRs using carbide and nitride fuel are presented. The assumptions used in the nuclear, thermal and mechanical designs are discussed together with geometry constraints, operational constraints, performance constraints, constraints coming from fabrication consideration and fuel bundle-duct interaction constraints. The basic calculational flow for system design studies is described, and the computer codes used in the analyses are briefly reviewed.

# The Breeding Performance of Carbide and Nitride Fuels

in 2000 MWe LMFBRs

- A Preliminary Report -

W. P. Barthold

## I. INTRODUCTION

The mixed oxide (U,Pu)O<sub>2</sub> has been selected as the fuel for FFTF as well as the first demonstration and commercial LMFBR. Its technology is well developed and its behavior under irradiation is largely understood.

Mixed carbide and nitride fuels promise higher breeding ratios and lower doubling times<sup>1-3</sup> because of the following properties

- (a) The thermal conductivity for carbide and nitride fuel is more than eight times the conductivity of oxide fuel. Since the melting points for carbide and nitride fuels are only slightly below that for oxide fuel they afford easily linear heat ratings which are significantly above that for oxide fuel. This can lead to a reduction in the required fissile inventory.
- (b) Carbide and nitride fuel show about a 33% higher heavy atom density than oxide fuel. Furthermore, they have only one moderating atom per heavy metal atom, compared to oxide fuel which has two. This results in a harder neutron spectrum and a better breeding ratio.

But while it is generally accepted that mixed carbide and nitride fuels in fast reactors are capable of a breeding performance superior

to that of mixed oxide fuel it is also recognized that a one-by-one substitution of carbide and nitride fuel for oxide fuel does not assure this superiority. The higher density of the fuels and the capability of high linear heat ratings require different designs to fully utilize the inherent advantages of mixed carbide and nitride fuels.

This series of reports is a preliminary assessment of the breeding performance of carbide and nitride fuels in 2000 MWe LMFBRs. The preliminary nature of this assessment is a reflection of the lack of data related to the irradiation behavior of these fuels. Both types of fuel were either sodium- or helium-bonded to the cladding. This series of reports summarizes a preliminary assessment of the breeding potential of advanced fuel, its sensitivity to changes in design and performance parameters, various design trade-off studies as well as special problems connected with the design of large LMFBRs.

This first volume summarizes the assumptions and constraints used throughout this study and it describes the methodology employed for the performance and design analysis.

## II. SCOPE AND LIMITATIONS

Reactor system studies were carried out employing carbide and nitride fuels. The system studies include determination of the sensitivity of breeding performance to variation in reactor core design parameters, evaluation of control and stability problems of medium vs. large LMFBRs, design optimization and assessment of optimization criteria and their impact on design. At this stage, no consideration was given to the

balance of plant nor were detailed designs developed. This work concentrated on an assessment of the breeding potential measured by a compound system doubling time (Appendix A). The impact on optimized breeding performance of using different performance measures like (doubling time \* specific inventory) (Appendix B) and fuel cycle cost, was analyzed, too. It is shown in Appendix B that the product of doubling time times specific inventory is a measure for the uranium ore requirement. But while this seems to be a convenient figure of merit, it must be remembered that it is derived from a simple economy model which assumes that at the time the installed nuclear capacity reaches a size necessary to assure that a self-sustained breeder system can be maintained, exactly this number of breeder reactors will be installed and for the future, no other reactor type will be installed.

Fuel cycle cost was not used as the main objective function in the performance studies and optimizations. It is felt that the uncertainties in cost data are currently too great to justify the development of cost-optimized designs. In designing the reactor, a conservative approach was used allowing only small extrapolation from current technology. Though these fuels would not be used in commercial reactors before the late 90s, at which time the LMFBR technology is expected to be more advanced than today, a conservative approach in design and analysis was preferred in an attempt to discount the common experience that the expected reactor performance is usually getting worse as more is known about the system and as more detailed design work is carried out. Whenever design assumptions had to be made for

which there was no good data base (for example, achievable smeared densities for various burnups in helium- and sodium-bonded pin designs) extensive sensitivity studies were carried out to assess the significance of the uncertainty.

The structural material used was 20% CW316SS. This is a limitation not based on an expected superiority of this material over other structural materials but is a reflection of the lack of material data for other structural materials at the time this study began. In the meantime swelling and creep data for other alloys were published and their impact on breeding performance will be assessed at a later time.

### III. ASSUMPTIONS AND CONSTRAINTS

#### A) Assumptions

To provide a consistent basis for an assessment of the breeding performance of carbide and nitride fuels, various assumptions were made with respect to the nuclear, thermal and mechanical design of the 5000 MWt LMFBRs as well as with respect to the material behavior and material properties. Tables I to IV show these assumptions which were the basis for the core design analysis.

The assumptions on the nuclear design are summarized in Table I. A fuel cycle length of 300 full power days was chosen for simplicity's sake and not to infer that 82.19% will be the ultimate plant capacity factor or that semi-annual or 18 months refueling cycles are inconceivable. A two-year residence time for fuel assemblies was selected for all pin diameters as a basis. The residence time for the blanket

Table I. Nuclear Design Assumptions

Total power, MW	5000
Total power peaking factor	1.65
Radial power peaking factor	1.375
Core height, ft.	3
Axial blanket length	
Upper axial blanket, in.	15
Lower axial blanket, in.	15
Axial reflector, in.	5
Rows of radial blankets	1
Blanket composition	CRBR
Control assembly composition	CRBR
Pin array	triangular
Number of pins/fuel assembly	169
Cycle length, fpd	300
Fuel residence time, fpd	600
Radial blanket residence time, fpd	1200
Number of control rods	12-36
Volume ratio inner core to outer core zone	~60/40

assemblies is 4 years as a basis. The sensitivity of the breeding performance to fuel residence time was determined separately. The 5000 Mwt size was selected as the reference size for LMFBRs in the late 1990s based on Reference 4. The current reactor size limit of 3750 Mwt was imposed to halt an escalation in reactor size and not because of anticipated technical problems. No arbitrary fluence limit was imposed since conclusions related to the breeding performance are then tied to an arbitrarily established limit and would change when this limit is raised or lowered. To keep the assembly size below 8 in., the number of fuel pins per assembly was limited to 169. The number of control rods varied from 12-36 depending on the excess reactivity requirements. The control rods were added to the core in groups of three assemblies to maintain symmetry. A total nuclear power peaking factor of 1.65 and a radial power peaking factor of 1.375 were assumed. While the actual power peaking factor for the reactors subject to the various design assumptions made will depend on pin size and fuel rating, an accurate prediction of power peaking factors is extremely difficult and requires detailed three-dimensional analyses. It has been shown that 2-D results for radial power peaking factors can be very misleading, <sup>(5)</sup> in particular when based on r-z geometry calculations. Cores with small-diameter fuel pins usually show lower power peaking than cores with large-diameter fuel pins when the analysis is limited to uncontrolled cores. However, cores with small-diameter fuel pins have larger reactivity losses during burnup than cores with large-diameter fuel pins, thus requiring more control rods. This in turn will tend to

increase the power peaking factor for the cores with small-diameter fuel pins. Therefore, no use was made of the power peaking factors which resulted from 2-D analyses of uncontrolled cores and a constant power peaking factor was assumed instead. Enrichment splits were determined such that power peaks in the two enrichment zones were the same at mid-equilibrium-cycle conditions. Two radial enrichment zones were used as a baoc. The impact of an increase in the number of radial enrichment zones was studied.

The thermal design assumptions are summarized in Table II. The coolant enters the core at 750°F and leaves it at 1050°F. Later studies use an inlet temperature of 720°F and a mixed mean outlet temperature of 1000°F. The maximum sodium velocity was limited to 25 ft/sec, though the impact of higher velocity limits and pressure drop constraints rather than coolant velocity constraints on breeding performance was analyzed, too.

The subchannel pressure drop for wire-wrapped fuel bundles was estimated taking into consideration the frictional and spacer losses following the method by Novendstern.<sup>(6)</sup> The calculation of the pressure drop in gridded fuel bundles was based on design equations supplied by Westinghouse-ARD (Ref. 7). No attempt was made to determine assembly inlet and exit losses as well as losses outside the core (piping, IHX, etc.). The thermal conductivities for mixed carbide and nitride fuel needed for the calculation of fuel and cladding temperatures were based on the data recommended by Washington.<sup>(8)</sup>

The assumptions made for the mechanical design of the core are summarized in Table III. The structural material used for the cladding and

Table II. Thermal Design Assumptions

Reactor inlet temperature, °F	750
Reactor mixed mean outlet temperature, °F	1050
Max. sodium velocity, ft/sec	25
Ratings for sodium-bonded fuel, kW/ft	25, 30, 35*
Ratings for helium-bonded fuel, kW/ft	14.81, 18.52, 22.22
Spacer concept	wire-wrapping, grids

\*Maximum nuclear linear heat ratings.

Table III. Mechanical Design Assumptions

Fuel pin diameter, in.	0.3, 0.35, 0.4, 0.45
Cladding thickness	
Helium-bonded fuel, in.	calculated*
Sodium-bonded fuel, in.****	0.015
Bond thickness	
Helium-bonded fuel, in.	0.005
Sodium-bonded fuel, in.	0.010 (minimum)
Core fuel pellet density, % T.D.	95
Cladding material	20% CW316SS
Duct material	20% CW316SS
Duct thickness	calculated**
Interassembly gap	calculated***
Fuel pitch	triangular
Duct shape	hexagonal
Stress limit on duct, psi	15,800
Strain limit on cladding (thermal component), %	0.5
Plenum length	
Sodium-bonded fuel, in.	30
Helium-bonded fuel, in.	40
Plenum location	bottom, top
Sodium-bonded fuel	top
Helium-bonded fuel	bottom

\*The cladding thickness was assumed to be proportional to the pin diameter with a reference pin of 0.31 in. and a cladding thickness of 0.20 in.

\*\*Determined such that the duct wall stresses stay below the stress limit.

\*\*\*Allowance was calculated for swelling, creep and handling

\*\*\*\*Includes 0.003 in. thick perforated shroud around fuel pellets.

assembly duct is 20% CW316SS. The fuel pins are arranged on a triangular pitch and are surrounded by a hexagonally shaped duct. For most analyses a pellet fabrication density of 95% T.D. was used. Later analyses of sodium-bonded carbide fuel used a 98% T.D. pellet density. In designing the fuel pin it was assumed that the fission gas plenum is located at the bottom of the fuel pin for helium-bonded fuel and at the top for sodium-bonded fuel. It is 30 in. long for sodium-bonded fuel and 40 in. long for helium-bonded fuel. While these choices are not meant to represent optimum dimensions the difference in length, which affects only slightly the pressure drop and therefore duct and interassembly gap size, is justified because of the differences in fuel operating temperatures and therefore fission gas releases, as well as fission gas pressure.

As of lately questions have been raised as to the usefulness of a bottom plenum versus a top plenum (Ref. 9). Though a bottom plenum could lead to a reduction in fuel pin length because it is located at a low-temperature position, the overall length of the core could increase. Control rods in their parked position sitting just above the core region would require the same height above the core as in case of the top-plenum fuel assembly. This could lead to an increase in overall core height. Furthermore, switching from helium-bonded to sodium-bonded fuel for a given design could be more easily accommodated when the fission gas plenum is located at the top. However, while the location of the fission gas plenum is of great importance for an actual design, an assessment of the breeding potential is not strongly affected by this choice.

The pitch-to-diameter ratio was not a design parameter but a derived

quantity. Sodium-bonded fuel was designed such that there was no fuel-cladding interaction at end-of-life condition. A constant cladding thickness of 0.015 in. was selected for the pin diameters selected which ranged from 0.3 in. to 0.45 in. This is an effective cladding thickness since it includes approximately 0.0015 in. in thickness coming from a 0.003 in. perforated shroud surrounding the pellet. In case of helium-bonded fuel, the cladding thickness increased proportionally to the pin diameter to keep the hoop stresses constant. Both wire and grid spacers were used. The selection of either spacer concept was based on consideration of maximum allowable wire thickness and spacer volume fraction. In general, the spacer volume fraction should not exceed significantly 2% of the total core volume and the wire thickness should stay below 0.120 in. The design of the grids was based on data provided by W-ARD (Ref. 7). The duct wall thickness was calculated such that the highest stresses in the duct wall stayed below the maximum allowable stress. The interassembly gaps were determined such that fuel pin and assembly duct had the same lifetime. A fuel assembly handling allowance was added to this interassembly gap to assure that the fuel assemblies at end-of-life can be withdrawn easily. This approach differs from the widely used "kiss-of-death" design basis whereby the fuel assemblies are touching at end-of-life conditions. But it was felt that the uncertainties in material, swelling and creep properties justify a more conservative design approach.

The bond thicknesses of 0.005 in. for gas-bonded and 0.010 in. for sodium-bonded fuel pins were based on information obtained from an early

ression of LASL (Ref. 10). Helium-bonded pin designs were based on results from an early version of the UNCLE code (Ref. 11). Since the resulting fuel smeared densities were substantially higher than the available experimental data could support, an extensive sensitivity study was conducted to assess the impact of changing smeared densities on the breeding potential.

The material properties used in these analyses are listed in Table IV. The swelling correlation for carbide fuel was based on a preliminary analysis of EBR-II swelling data. The nitride fuel swelling was assumed to be the same as that for carbide fuel.

#### B) Constraints

The optimization of reactor performance with respect to a performance index requires the analysis of various reactor designs which satisfy design constraints. A comparison of the performance of different reactors requires that these reactors satisfy the same set of constraints. It is sometimes debated if design constraints should be applied at the beginning of the design work or at a later stage as a means to screen different results. But using constraints only to screen designs and their analysis does not eliminate attacks on problems which are only of academic interest at best. It is certainly not meaningful to overconstrain the design but it is equally meaningless to apply no constraints at all. (14)

There is little disagreement among reactor designers that the application of design constraints is very useful. For one, the constrained design approach limits the number of designs which need to be analyzed and secondly, this approach assures the feasibility of designs by using an integrated design approach. The disagreements on the usefulness of the

Table IV. Material Behavior and Material Properties

## Density

UC-PuC, gm/cc	13.60
UN-PuN, gm/cc	14.32
SS316CW, gm/cc	7.941
Na, lb/ft <sup>3</sup>	53.5

## Thermal conductivity

UC-PuC, Btu/hr-ft-°F	9.7*
UN-PuN, Btu/hr-ft-°F	7.8*
SS316CW	12.5

Specific heat for sodium, Btu/lb-°F 0.306

## Swelling correlations

Nitride, carbide fuel<sup>(12)</sup>

$$\frac{\Delta V}{V} = B \exp [9 \cdot 10^{-4} (T_c - 800)]$$

Swelling Correlations for Cladding and Structural Alloys (Reference 13)

For 20% CW Type 316 stainless steel:

$$\frac{\Delta V}{V_0} = R \left\{ \phi + \frac{1}{\alpha} \ln \left[ \frac{1 + \exp \alpha (\tau - \phi)}{1 + \exp (\alpha \tau)} \right] \right\}$$

where  $\Delta V/V_0$  = stress-free swelling in percent

$\phi$  = neutron fluence ( $E > 0.1$  MeV) units of  $10^{22}$  n/cm<sup>2</sup>

T = irradiation temperature, °C

R = exp B

\*at 1000°C for 100% T.D. (8)

Table IV. (contd.)

$$B = -88.5499 + 0.531072T - 1.24156 \times 10^{-3} T^2 \\ + 1.37215 \times 10^{-6} T^3 - 6.14 \times 10^{-10} T^4$$

$$\tau = 257.262 - 2.39381T + 8.16677 \times 10^{-3} T^2 \\ - 1.18508 \times 10^{-5} T^3 + 6.21367 \times 10^{-9} T^4$$

and

$$\alpha = -1.11667 + 6.88889 \times 10^{-3} T.$$

constrained design approach come from the difficulties to quantify constraints. Earlier design work used an empirical design approach. Experience obtained either in the operation of similar reactors, in irradiation experiments, in the manufacturing area, etc., provided constraints for the design. As our knowledge about reactors grew, the empirical approach gave way to a deterministic approach. The core designer, for example, did not just use the recommendation made by the fuels experts as to the maximum obtainable linear heat rating, based on irradiation experience, but he introduced the fuel melting as a criterion for the design and calculated the obtainable rating. For conservatism in design he then designed the fuel pin such that the fuel centerline temperature stayed below the melting temperature by a given margin. Fuel pins were designed to achieve a certain burnup by quantifying gas release, fuel and clad temperature history, fuel and clad swelling, allowable strain levels, etc. The feeling was then that quantifying design parameters by using material properties eliminates the arbitrariness introduced in the empirical design approach. But it did not take long and the designer was asking about the uncertainties in material properties, etc., and how they affect design and performance parameters. For example, if a pin is designed for a certain maximum allowable burnup, this does not mean that all pins will fail when they exceed this burnup. The design techniques were modified to determine a fuel pin design such that less than a certain percentage of the fuel pins will fail with a certain probability when the nominal burnup limit is exceeded. Maximum allowable power ratings are determined such that there is a certain probability that not more than a

certain volume of a fuel pellet will melt. While these probabilistic approaches seem to be intrinsically superior to the deterministic or empirical approaches in design, somebody has to tell the designer what "acceptable probabilities" are. At this point, however, the design approach turns back to judgements for guidance. These judgements are probabilities and confidence levels rather than hardware-related experiences. One has to keep in mind that all three design approaches rely ultimately on judgement and a probabilistic approach is not necessarily superior to an empirical approach. Another limitation in the probabilistic approach comes from the requirement that uncertainties in material properties and other input data to a probabilistic assessment have to have a statistical significance. In most uncertainties this will be very difficult to prove. An example is the swelling correlation for 20% CW316SS. The scatter of the basic data from which the correlation is derived is very wide. In addition, there are possibilities for biases since some data are derived from actual neutron irradiation, others from ion bombardments. Furthermore, the expected range of validity of such a swelling correlation extends far beyond the fluences ever observed. Under these circumstances, it is impossible to define a meaningful statistically significant uncertainty. Furthermore, one has to keep in mind that design constraints are not absolute but have to represent a compromise. Constraints applied to LMFBR designs are derived from the premise that a breeder reactor has to breed, and produce power safely and economically. It is easy to enhance the safety of a reactor by overdesigning the reactor. But overdesign of

the reactor affects adversely economics and breeding. Enhancing the safety of a reactor, for example by spoiling the core geometry, usually leads to penalties in economics and breeding. Making a reactor more economical by increasing the fuel residence time usually penalizes breeding performance and safety. Improvements in the breeding performance are usually connected with penalties in the economics and often also penalties in safety. Going to shorter residence times of the fuel will usually improve breeding but hurt the economics. Reducing design margins to reduce the amount of structural materials in the core and increasing the fuel linear heat rating will improve the breeding characteristic of the reactor but also reduce safety margins.

The designer therefore has to weigh breeding, economics and safety features of the reactor and reach a compromise. This compromise will be reflected in the design constraints he applies.

In the following, constraints will be discussed which were used and can be applied in designing the advanced fuel LMFBR cores. Some of these are based on core geometry consideration, others are based on performance limits which are often derived from material properties. Examples are pressure drop limits, rupture life limits, maximum clad temperatures, etc. An additional group of constraints is derived from limitations imposed on the design but not related to material properties. Examples are fuel cycle cost, power cost, doubling time, etc. which have to stay below certain limits.

a. Geometry Constraints

Optimum reactor performance requires a symmetric core layout. In case of hexagonal fuel assemblies, the number of positions for fuel assemblies in a core layout of regular hexagonal shape is given by

$$3n(n-1) + 1$$

for  $n$  rows of fuel assemblies. By removing three assemblies at each corner of the hexagon in order to obtain a more circular periphery the number of assemblies for  $n$  rows of assemblies becomes

$$3n(n-1) - 17$$

$$n > 3$$

Since the control assemblies have to be arranged in a way that they span a hexagon, the number of positions for fuel assemblies is given by

$$\left. \begin{array}{l} 3n(n-1) + 1 \\ 3n(n-1) - 17 \end{array} \right\} - \left\{ \begin{array}{l} (6N+1) \\ 6N \end{array} \right. \quad \begin{array}{l} \text{control assembly at core} \\ \text{center position} \\ \text{fuel assembly at core} \\ \text{center position} \end{array}$$

with  $N$  . . . . number of rings of control assemblies.

The variety of core arrangements can be increased slightly by arranging the control rods in a way that they span a triangle. This arrangement would tend to decrease the self-shielding of the control rods.

## b. Performance Constraints

### 1. Pressure Drop

For single-stage mechanical impeller pumps, the maximum allowable system pressure drop is limited to less than 200 psi. Limits on pin bundle pressure drop are usually set below 100 psi. A 90 psi limit was used in the advanced fuel system studies.

### 2. Maximum Clad Temperature

A clad temperature limit of 1350°F or 1400°F including HCFs is often used as a design limit. The clad temperature in itself is not a real constraint since it is important only insofar as it affects the fuel pin lifetime (rupture life). But for a given fuel pin design which was based on a certain fluence, burnup and temperature condition the cladding temperature limit is a true constraint. For the advanced fuel LMFBRs cores analyzed in this series of reports, cladding hot spot temperatures ( $2\sigma$ ) were always below 1350°F.

### 3. Fuel Pin Rupture Life

For any design, the performance analysis is only valid if the calculated time to failure of the pin is greater than its residence time. While this seems to be a very valid constraint, its mathematical formulation is quite difficult. For one, a rupture life correlation is necessary which describes the rupture life as a function of internal pressure and temperature. Secondly, one needs to know what the internal pressures are coming from fission gas build-up and fuel-cladding interaction, the latter being extremely important but also difficult to describe mathematically.

Currently, fuel lifetimes codes and empirical correlations are being used for the prediction of fuel rupture life.

#### 4. Maximum Sodium Velocity

While the maximum allowable pressure drop can often limit the maximum allowable sodium velocity, the sodium velocity is also limited because of cavitation and to a lesser extent corrosion. There are no exact limits on the sodium velocity but it is generally agreed that the maximum sodium velocity in the fuel bundle should not exceed 40 ft/sec. For design applications this limit is often placed at much lower velocities.

#### 5. Duct Stresses

The stresses in the ducts are usually the highest at the bottom elevation of the fuel assembly with the greatest pressure. The stress limits for the materials considered are used to determine the minimum duct wall thickness.

#### 6. Power-to-Melt

To avoid fuel melting, several approaches are being used to determine limits on the linear heat rating. The approach used in this series of reports is to constrain the fuel centerline temperature to be always below the melting point by 100°F. Another approach could be a statistical interpretation of the fuel melting limit. A probability for melting of a certain fraction of the peak power pellet can be determined. The latter approach though inherently very powerful has the disadvantage of nearly all statistical approaches to reactor design and safety, namely the difficulty in the definition of statistically meaningful uncertainties.

In both approaches, the power-to-melt criterion has to be applied to the average power times nuclear power peaking factors (including the uncertainty in the calculation) times an overpower factor (usually 1.1-1.15).

c. Constraints Coming from Fabrication Considerations

Examples for constraints coming from manufacturing tolerances are diametral gaps both for helium- and sodium-bonded fuel (see Table III), lower limits for clad thicknesses (0.010 in.), and achievable fuel densities (98% T.D. maximum pellet density for carbide and nitride fuel). For wire-wrapped fuel, there is a range of feasible p/d ratios. Limits come from both low as well as high p/d ratios. Because of the high linear heat rating for carbide and nitride fuel, low p/d ratios are not limiting for core fuel assemblies because the spacer wire thickness is seldom less than 0.045 in. However, wire wrapping was not used as a spacer concept whenever the spacer wire thickness exceeded 0.120 in. For certain design analyses, the constraint on the spacer concept was that a spacer volume fraction should be equal or less than 2%.

d. Operational Constraints

From the core designer's point of view, inlet and outlet temperature and mixed mean coolant temperature rise are often constrained by considerations of thermal stresses under steady state as well as transient conditions. They depend on design details and are usually difficult to quantify (thermal shock on upper internals and vessel outlet, stresses due to large temperature differences at the outlet of adjacent fuel assemblies, etc.). In this series of reports no attempt was made to quantify these constraints.

The operational cycle length was limited to 300 full power days. Ultimately, this constraint has to reflect a utility's desired mode of operation. In this series of reports, the impact of 150 fpd and 450 fpd cycles on the breeding performance will be discussed, too.

e. Fuel Bundle-Duct Interaction Constraints

The obtainable duct life time has been constrained so far only by the available space between fuel assemblies and the stress level in the duct wall due to the coolant pressure. Another important parameter affecting the duct life is the fuel bundle-duct interaction.<sup>(15)</sup>

The outermost row of fuel pins inside a fuel assembly is usually over-cooled. This leads to duct temperatures which can be well below the average clad temperature inside the fuel assembly. Therefore, cladding and the duct will swell at different rates and the fuel bundle will ultimately mechanically interact with the duct wall. This could be considered the life limit for the duct. At this time, however, not enough analysis has been carried out to take properly into account dispersion and enhanced duct swelling due to increased duct wall temperatures which are a result of the reduction in the hydraulic diameter of the outermost row of fuel pins due to bundle compression. Furthermore, the limiting fuel bundle-duct interaction can be delayed by enhancing duct swelling which can be achieved by having the outermost row of fuel pins double-wrapped in order to reduce the flow area. For these reasons, the duct life calculations for system studies were not constrained by bundle-duct interaction.

Design studies can also be constrained by expected performance parameters, for example, compound system doubling time, fuel cycle and plant costs. These constraints, however, are to some extent arbitrary. Other constraints could be sodium void reactivity, Doppler coefficient, expansion coefficient, etc. Though each of these parameters is important for safety consideration, at this time it is not possible to identify quantitatively what the magnitude of these safety parameters has to be.

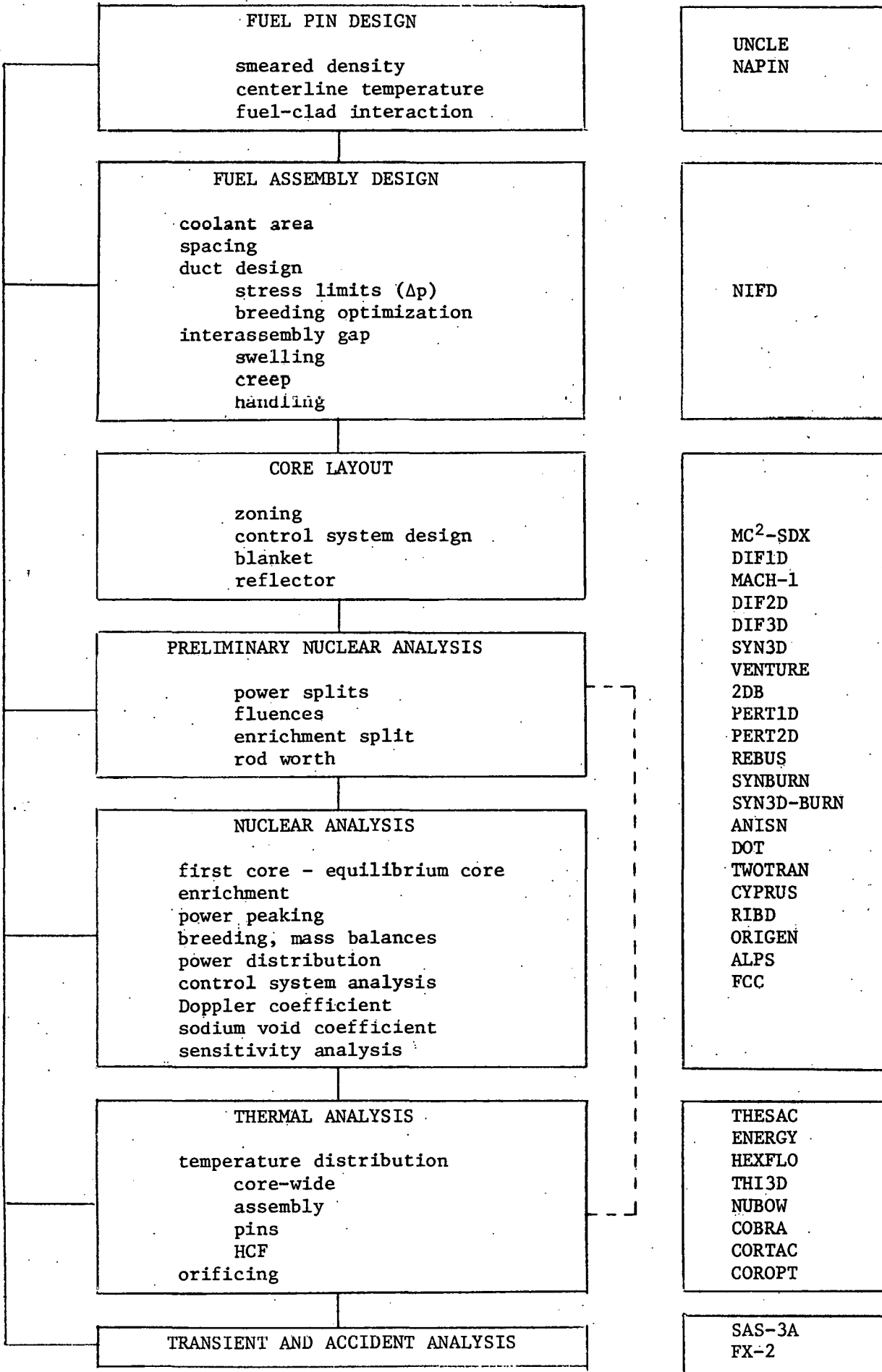
None of these constraints were used in the studies described in this series of reports.

#### IV. METHODOLOGY FOR DESIGN AND ANALYSIS

The major characteristic of system design analysis is that it is an analysis which links nuclear, mechanical and thermal design to obtain consistent core designs. A constrained design approach is necessary to optimize cores with respect to certain performance indices. The application of constraints limits the number of designs which have to be evaluated to optimize a performance index. Examples for design constraints are maximum sodium velocity, coolant temperature rise, stress limits for ducts, cumulative damage fraction, limiting power-to-melt, maximum allowable pressure drop, total inelastic strain due to thermal and irradiation creep, etc. Examples for performance indices which can be optimized are compound system doubling time (Appendix A), doubling time times specific inventory (Appendix B), fuel cycle cost, power generating cost, etc.

The system design approach currently used is discussed in the following. Table V shows the basic calculational flow for system

Table V. Basic Computational Flow for System Design Studies



design studies and the computer codes used. The system design begins with the fuel pin design and continues from there with the fuel assembly design and core layout. A preliminary nuclear analysis of the core layout provides feedback to the fuel pin design, assembly design and core layout. After the designs converged more detailed nuclear and thermal analyses are following. Transient and accident analyses complete the design analysis although for most system studies this type of analysis will only be carried out for otherwise optimized designs. Results from transient and accident analyses which were performed in the past are used as a guidance to the core design efforts.

The fuel pin design is the first step in the system analysis. For a given pin diameter, cladding thickness and fuel material density have to be known as a function of operating conditions, i.e., temperature, pressure drop, burnup, fluence, residence time.

An early version of the UNCLE code was used to design helium-bonded carbide and nitride fuel pins. The cladding thickness is derived from a reference fuel pin design by keeping the hoop stresses the same, i.e., the ratio of cladding thickness to pin diameter is held constant (wastage allowances are taken into account). The UNCLE code calculation, however, gave smeared densities which were substantially higher than expected based on experimental data.<sup>(16)</sup> Therefore, in addition to the fuel pins derived directly from UNCLE, extensive sensitivity studies were conducted to determine the impact of fuel density on breeding performance.

Sodium-bonded carbide and nitride fuel pin designs were derived from the NAPIN<sup>(17)</sup> code which is a simplified version of UNCLE and

uses the basic swelling characteristics of these fuels and the cladding.

The cladding thickness for sodium-bonded fuel was fixed at 0.015 in.

for CW316SS. (18)

Another approach to fuel pin design would be to select smeared density, cladding thickness and operating condition and determine a fuel lifetime based on, for example, the cumulative damage fraction concept. In this case, however, one has no guarantee that the resulting fuel lifetime is a multiple of a selected burnup cycle. Because of this ambiguity we determined fuel pin designs such that they also satisfy this constraint.

In designing fuel pins, fluence and burnup information as well as hot channel factors are needed. Data from previous analyses are taken as a first guess.

In reviewing the fuel irradiation data it is difficult to see clear trends in fuel swelling as a function of temperature, burnup and fluence. It could then be argued that perhaps a constant smear density independent of operating condition might be a better choice for system studies and that the designs and their analysis should be carried out for several smear densities. This approach was not used for the following reasons. The constant smear density approach increases the number of cores which have to be analyzed by a factor of 2-3 (using 3 or 4 different smear densities) which is physically difficult but possible to analyze. The major problem, however, is: what is the meaning of all these data? It is known that lower smear densities will lead to poorer breeding performance. One would therefore not lower the smear density of a pin design unless there are also benefits to be obtained. To derive any conclusion from this wealth of data obtained using this approach, judgment needs to be applied as to a possible change in smear den-

sity as a function of burnup and/or temperature (fuel and/or clad). This judgment, however, is better applied at the beginning of the analysis to limit the number of cores which have to be designed and analyzed rather than at the end.

The next step in the analysis is the design of the fuel assembly for which the NIFD code<sup>(19)</sup> is being used. Input data are coolant inlet and outlet temperature, maximum coolant velocity, maximum linear heat rating, core height and blanket thickness, fuel pin diameter, reactor power and power split, stress limits and fast fluence. Output data are fuel pitch-to-diameter ratio, duct wall thickness, duct inside flat-to-flat distance, required interassembly gap as a function of axial position (allowing for swelling, irradiation creep and handling), number of fuel assemblies needed, bundle pressure drop, and volume fractions. The code can handle both wire-wrapped as well as gridded assemblies. Based on the number of required fuel assemblies and the estimated number of control positions, the code also determines the actual number of fuel assemblies for a hexagonal core layout where the corners can be rounded off, if needed.

One of the critical issues in this analysis is the calculation of duct wall thickness and the interassembly gap. Based on previous physics analysis, in most cases the optimum duct wall thickness  $T$  is calculated such that it satisfies the following equation

$$\sigma^{\text{limit}} = \Delta p \left( a \left( \frac{L_F}{T} \right)^2 + b \left( \frac{L_F}{T} \right) \right) \quad (1)$$

with  $\Delta p$ ...pressure drop,  $L_F$ ...distance across the assembly flats,  $\sigma^{\text{limit}}$ ... stress limit for the material under consideration,  $a, b$ ...constants. After

the duct wall thickness is calculated, the interassembly gap is calculated such that both assembly duct and fuel pins have the same lifetime (Appendix C). In case of some advanced alloys, however, it was found that a duct wall thickness derived from Eq. (1) led to very large duct rounding due to irradiation creep and the optimization of the breeding performance required an increase in duct wall thickness to reduce the interassembly gap. Because of this finding it is always checked if the duct wall thickness derived from Eq. (1) assures optimum breeding performance or if the duct wall thickness needs to be increased.

Based on the pin design data, core size and core and blanket volume fraction, nuclear cross section sets are being prepared.

The MC<sup>2</sup>-2-SDX<sup>(20)</sup> code system is used to determine heterogeneously or homogeneously self-shielded nuclear cross sections for core and blanket regions based on ENDF/B Version IV microscopic nuclear cross section data. The code allows space- and energy-collapsing of cross sections.

For burnup analysis, 8-group cross sections are usually used. For sodium-void and Doppler calculations, 21 group cross sections are in use. Separate cross section sets are prepared for oxide, carbide and nitride cores and they are used for a variety of pin designs. Separate cross section data sets are prepared for three different temperatures as well as for cores with and without sodium.

The next step in the analysis is a refinement of the core layout which was obtained from NIFD. Based on extensive zoning analyses the volume ratio of inner to outer core region should be in the neighborhood of 60/40. Control rods are arranged on a hexagonal layout. Between one and three rows of

radial blanket assemblies surround the core. Outside the blanket region is the reflector region (both radially and axially).

The next step in the analysis is the preparation of a cylindrical model of the reactor which is used for preliminary nuclear analysis. The information needed at this stage is an update in the initial guesses on power splits, fluence, burnup, enrichment split, control rod worth and burnup swing. These data feed into the fuel pin design codes and the fuel assembly code NIFD. They are derived from the SYN BURN<sup>(21)</sup> code. SYN BURN is a 2-D synthesis burnup code which calculates beginning- and end-of-equilibrium cycle performance characteristics and mass balances.

Usually, there is only one iteration required between the performance guesses which feed into fuel pin and assembly designs as well as the core layout and the updated design and layout based on the preliminary nuclear analysis. What follows is the nuclear analysis in the detail consistent with the answers one is seeking. In general, one wants to know what the first core and equilibrium core performances are. Enrichment, power peaking, mass balances, power distribution, control system characteristics and design, safety coefficients are some of the data one is interested in. Sensitivity analyses are often part of the nuclear analysis.

In the nuclear analysis, the following codes are being used.

#### Diffusion Codes

For one-dimensional diffusion codes, the codes DIF1D<sup>(22)</sup> and MACH-1<sup>(23)</sup> are used. DIF2D<sup>(24)</sup> is available in r-z, r- $\theta$ , and hexagonal geometry and is routinely used with a large variety of search options. As of lately DIF3D<sup>(25)</sup> and SYN3D are also being used. The first code is an extremely fast 3-D code which uses only a fraction of the computer running time of VENTURE<sup>(26)</sup> code

which had been used before DIF3D became available. SYN3D<sup>(27)</sup> is a 3-D synthesis code which has great flexibility with regard to geometry options and trial functions to be used. PARC1D<sup>(28)</sup> and PARC2D<sup>(29)</sup> are one- and two-dimensional perturbation codes which are being used for worth calculations in general and sodium void and Doppler reactivity distribution in particular.

The REBUS<sup>(30)</sup> code package which performs burnup calculations in 1, 2 and 3D is routinely used. The code system handles discrete burnup, equilibrium cycle analysis, homogenized fuel management, discrete fuel management, fuel shuffling as well as a large variety of fuel recycle options. The SYNBURN code is a 2-D synthesis burnup code which handles equilibrium cycles. It does not offer options different from REBUS but is an extremely fast running code. The 2DB<sup>(31)</sup> code is available for burnup analysis but the preferred codes are REBUS and SYNBURN. A 3-D synthesis burnup code SYN3D-BURN<sup>(32)</sup> became recently available and will be used extensively in the near future.

#### Transport Codes

In use are ANISN,<sup>(33)</sup> DOT<sup>(34)</sup> and TWOTRAN<sup>(35)</sup> for one- and two-dimensional neutron and gamma transport calculations and the calculation of heat deposition.

#### Miscellaneous Nuclear Design Codes

The CYPRUS<sup>(36)</sup> code package is used for reactivity and power shape control analysis. The code determines the enrichment distribution in a multi-zone reactor such that a desired power shape is achieved at beginning-of-life condition. Furthermore, it calculates the poison distribution dur-

ing operation of the reactor such that the reactor remains critical and a desired power distribution is retained.

The RIBD code<sup>(37)</sup> and ORIGEN<sup>(38)</sup> code are used to calculate the fission product content of irradiated fuel and heating effects accompanying radioactive decay. The calculations follow the irradiation history including shutdown periods and operation at different power levels.

After completion of the nuclear analysis, core layout, fuel management, and power distribution feed into the thermal analysis. The codes HEXFLO, ENERGY and THESAC are the codes most often used.

The HEXFLO<sup>(39)</sup> code determines steady-state core-wide temperature distributions. It is based on the ENERGY<sup>(40)</sup> code and takes interassembly heat transfer into account. Fuel assemblies can be orificed individually. Coolant temperatures are calculated inside all fuel assemblies as well as duct temperatures and cladding hot-spot temperatures.

The ENERGY code determines the temperature distribution inside a fuel subassembly. The various mixing modes are lumped into an equivalent turbulent cross-flow which is described by an effective eddy diffusivity.

The THESAC<sup>(41)</sup> code does single channel analysis yielding temperatures for bulk coolant, inside clad and fuel centerline as a function of axial position. These calculations are restricted to the hottest channel in the subassembly. A hot channel factor analysis is included.

The results of this analysis provide feedback to fuel pin and assembly design, core layout and may require a modification of operating conditions. In most instances, a preliminary hot spot analysis is performed in advance of the fuel pin design. It is usually based on earlier calculations of

HCFs for similar pins. It is for this reason that the preliminary nuclear analysis is often followed directly by the thermal analysis and a more detailed nuclear analysis is carried out after the feasibility of the thermal design has been assured.

The thermal analysis of the reactor is followed by transient and accident analysis.

The SAS-3A<sup>(42)</sup> code is used for off-normal transient analysis together with FX-2,<sup>(43)</sup> a 2-D space-kinetics code which can also handle point kinetics.

To study the systems aspects of a given design the ALPS<sup>(44)</sup> code is used which optimizes an electric power generating system subject to a wide variety of constraints. For fuel cycle cost calculations several in-house developed codes are being used.

All the major design codes were modified such that they are compatible with each other, i.e., output from one code can be used directly as input to another code. In addition to these codes, there is available a large variety of utility codes for plotting, input preparation, format changes, output processing, doubling time calculations, etc. Various other codes like NUBOW<sup>(45)</sup> (thermal and irradiation induced bowing), THI3D<sup>(46)</sup> (3-D thermal-hydraulics of a fuel assembly), COBRA<sup>(47)</sup> (same), CORTAC<sup>(48)</sup> (core restraint transient code), COROPT<sup>(49)</sup> (core optimization code for oxide fueled LMFBRs) are used to address special problems. However, these codes were not used on a routine basis for the assessment of the breeding performance.

## V. SUMMARY

The design of LMFBR cores depends strongly on the assumptions and constraints which characterize and limit the core design and its performance. In deriving the design assumption, no attempt was made to project any future technology. Most assumptions reflect the current state-of-the-art. The structural material used was 20% CW316SS. This is a limitation which is not based on an expected superiority of this material over other structural materials, but is a reflection of the lack of material data for other structural materials at the time this study began. Future studies will also include other alloys whose material properties were published recently. The cores which have been analyzed use carbide and nitride fuel in either their sodium- or helium-bonded versions. The lack of sufficient irradiation data on these fuels made it mandatory to design these cores conservatively so that the calculated performance characteristics, especially the breeding characteristics, are not dependent on major technological breakthroughs. Great care was exercised to assure the feasibility of those cores by integrating nuclear, thermal and mechanical design. In selecting design constraints emphasis was placed on the simplicity of the constraints consistent with the purpose of the system studies, which is an assessment of the breeding performance of carbide and nitride fuels in 2000 MWe LMFBRs. Five groups of constraints were discussed: geometry constraints; performance constraints; constraints coming from fabrication consideration; operational constraints; fuel bundle-duct interaction constraints. Four of these constraints were employed in the design of the various cores. Preference was given to a deterministic

design approach over a probabilistic design approach.

The system design begins with the fuel pin design and continues from there with the fuel assembly design and core layout. A preliminary nuclear analysis of the core layout provides feedback to the fuel pin design, assembly design and core layout. After the designs converged more detailed nuclear and thermal analyses followed. In many instances the preliminary nuclear analysis is followed directly by the thermal analysis and a more detailed nuclear analysis is carried out only after the feasibility of the thermal design has been assured. Transient and accident analyses complete the design analysis, although for most system studies this type of analysis will only be carried out for otherwise optimized designs. Results from transient and accident analyses which were performed in the past were used as a guidance to the core design efforts.

A large arsenal of computer codes is in use for the nuclear, thermal and mechanical design analysis. The computer codes range from survey codes for scoping studies to larger computer code systems for detailed analysis. At this stage, no consideration was given to the balance of plant, nor were detailed designs developed. The work reported in this series of reports concentrated on an assessment of the breeding potential measured by a compound system doubling time. The impact on optimized breeding performance of using different performance measures like (doubling time \* specific inventory) and fuel cycle cost, was analyzed, too.

## APPENDIX A

## THE DEFINITION OF COMPOUND SYSTEM DOUBLING TIME

A. Basis Assumptions

1. All  $^{235}\text{U}$  above a base 0.2% is counted as fissile inventory which has to be doubled. If depleted uranium with 0.2%  $^{235}\text{U}$  is used as a diluent, this  $^{235}\text{U}$  content is not counted as fissile material.
2. The plutonium composition is that of LWR discharge plutonium with the following composition:
 

$^{239}\text{Pu}$	68.0%
$^{240}\text{Pu}$	19.4%
$^{241}\text{Pu}$	10.2%
$^{242}\text{Pu}$	2.4%
3. For the calculation of the  $^{241}\text{Pu}$  losses due to decay, a half-life of 14.7 years is assumed.
4. A fuel cycle loss factor of 1% is used.
5. An external cycle time of 1 year is used.

B. Basic Equation

The compound system doubling time, CSDT, is calculated according to

$$\text{CSDT} = 0.693 \times \frac{M_{\text{in}} + M_{\text{ex}}}{(G - L_{\text{p}} - L_{\text{d}}) \times \frac{\text{cycles}}{\text{year}}}$$

with

$M_{in}$  = In-reactor fissile inventory

$M_{ex}$  = External cycle fissile inventory

$G$  = Fissile gain/cycle

$L_p$  = Fuel cycle losses

$L_d$  =  $^{241}\text{Pu}$  decay loss for the external cycle

### C. Definition of Components

#### 1. In-reactor fissile inventory, $M_{in}$

The BOC (beginning-of-cycle) inventory is used as in-reactor fissile inventory, including in-core as well as blanket fissile inventories.

In case only MOC (middle-of-cycle) inventories are available, the BOC inventory is estimated by

$$\text{BOC} = \text{MOC} - \frac{1}{2} G$$

#### 2. External cycle fissile inventory, $M_{ex}$

The following expression is used for the calculation of the external cycle fissile inventory:

$$M_{ex} = M_{in} \times \text{R.F.} \times \frac{T_{ex}}{T_{cycle}}$$

with

R.F. = Refueling fraction

$T_{ex}$  = External cycle time

$T_{cycle}$  = Cycle length

For a multiregion refueling, an effective refueling fraction is obtained according to

$$M_{\text{ex}} = \sum_j M_{\text{in}}^j \times (\text{R.F.})^j \times \frac{T_{\text{ex}}}{T_{\text{cycle}}}$$

where the superscript  $j$  denotes the region, and

$$\sum_j M_{\text{in}}^j = M_{\text{in}}$$

### 3. Fissile gain, $G$

When an explicit depletion calculation is performed, the fissile gain over the equilibrium cycle naturally results. The depletion analysis is performed taking the  $^{241}\text{Pu}$  decay into consideration. When MOC static calculations are performed, the fissile gain is estimated by the breeding gain and the energy produced during the cycle. However, the following correction factors are included in this method.

- a) The ratio of fissile isotope fission to total fission.
- b) The ratio of fissile destruction to fissile fission.

In either method, the fissile gain is adjusted by the  $^{241}\text{Pu}$  decay loss during the cycle.

### 4. Fuel cycle losses, $L_p$

The fuel cycle losses (fabrication and reprocessing losses) are calculated according to

$$L_p = \text{EOC} \times \text{R.F.} \times 0.01$$

with

EOC = End-of-cycle fissile inventory

$$= M_{in} + G$$

5.  $^{241}\text{Pu}$  decay loss  $L_d$

The  $^{241}\text{Pu}$  decay loss for the external cycle is approximated by

$$L_d = M_{EOC}^{241} \times \text{R.F.} \times (1 - e^{-\lambda T_{ex}})$$

$$= M_{EOC}^{241} \times \text{R.F.} \times 0.04606$$

## APPENDIX B

## A FIGURE OF MERIT FOR ORE CONSERVATION

To measure the performance of a fast breeder reactor with respect to uranium ore conservation in a nuclear power system consisting of different types of reactors is a very complex task and requires detailed system studies. However, it is possible to determine a figure of merit for a breeder reactor in regard to ore consumption for an idealized nuclear power generating system. The problem can be stated as: how much uranium has to be mined in order to start out with a self-sustaining breeder reactor system? After the breeder reactor is installed, no other reactor types will be built. The condition for a self-sustained breeder system is that it produces enough excess plutonium to fuel all new reactors which have to be added to the power generating system. With  $G$ ... electrical growth rate (GWe/yr),  $DT$ ...breeder doubling time equalling  $1/Y$  with  $Y$ ...yield,  $SI$ ...breeder specific inventory (kg Pu/GWe),  $I$ ... total breeder inventory, we can write the condition for a self-sustaining breeder system as

$$I \cdot Y = G \cdot SI$$

or

$$I = G \cdot SI \cdot DT$$

We can write

$$I = K \cdot SI$$

with  $K$ ...required breeder capacity to assure that self-sustained breeder systems can be maintained which can also be expressed as

$$K = G \cdot DT$$

To accumulate  $I$  in order to install  $K$  breeder reactors at one time, converter reactors are needed. If  $C$  measures the conversion of natural uranium into plutonium

$$C = \frac{\text{kg nat. U}}{\text{kg Pu}}$$

one can express the total ore requirement  $Q$  as

$$Q = I \cdot C$$

or

$$Q = G \cdot SI \cdot DT \cdot C$$

In this equation,  $SI \cdot DT$  are breeder-design related and therefore, the product of

$$SI \cdot DT$$

can be used as a figure of merit of a breeder reactor with respect to uranium ore requirements. The smaller the product of  $SI \cdot DT$  is, the lower are the uranium ore requirements.

While this is an easily accessible parameter in the characterization of a fast reactor, it must be remembered that it is derived from a simple model which assumes that at the time the installed nuclear capacity reaches  $G \cdot DT$ , exactly this number of breeder reactors will be installed

and for the future, no other reactor type will be installed. Actual system studies allowing a mix of different reactor systems might therefore show slightly different results with respect to breeder reactor optimization to reduce ore requirements.

## APPENDIX C

## CALCULATION OF INTERASSEMBLY GAPS (DUCT DILATION) (50,51)

In order to accommodate duct diametral dilation due to irradiation-induced swelling and creep, the reactor must be designed with sufficient space between the subassemblies to assure their structural integrity and to permit their removal at the end of life.

A. Introduction

The required gap  $g$  between ducts in an LMFBR to compensate for duct dilation can be estimated by using the expression:

$$g = L_F \chi / (L_F + 5\chi) \\ + (L_F + 2T)(\% \Delta V / V) / 300 \quad (C1) \\ + 0.0131 (L_F + 2T)$$

where

$$\chi = 0.00695 \Delta P \frac{L_F^4}{T^3} \text{ K.} \quad (C2)$$

The three terms in the expression for  $g$  represent, respectively, (a) duct rounding due to irradiation-enhanced creep from internal pressure, (b) duct dilation due to swelling, and (c) allowance for handling and bowing.

B. Derivation

(1) Duct Rounding. It is assumed that rounding which results from inelastic strain is identical to that which would result from the same amount of elastic strain. The latter rounding is obtained from the

conventional equation for elastic deformation of a beam with fixed ends and uniform load:

$$f = \frac{1}{384} \frac{W_{\text{art}} \ell^4}{EI} = \frac{1}{384} \frac{W_{\text{art}}}{E} \ell^4 \frac{12}{T^3} \quad (\text{C3})$$

where  $W_{\text{art}}$  is an artificial unit load which produces an amount of elastic strain, near the ends of the beam, which equals the circumferential inelastic strain near the corners of an actual duct. To express Eq. (C3) in terms of strain rather than  $W_{\text{art}}$  it is convenient to introduce  $\sigma_{\text{art}}$ , an artificial stress corresponding to the elastic strain:

$$\sigma_{\text{art}} = \frac{Mc}{I} = \frac{1}{12} W_{\text{art}} \ell^2 \frac{T}{2} \frac{12}{T^3} = \frac{W_{\text{art}}}{2} \left(\frac{\ell}{T}\right)^2 \quad (\text{C4})$$

But,  $\sigma_{\text{art}} = \epsilon E$ , and

$$\ell = L_F / \sqrt{3}$$

so that, from Eq. (C3)

$$f = \frac{24}{384} \frac{L_F^2}{3T} \epsilon = 0.0208 L_F^2 \epsilon / T \quad (\text{C5})$$

The inelastic strain comes from

$$\epsilon = K\sigma \quad (\text{C6})$$

where

$$\sigma = \frac{1}{2} \Delta P \left(\frac{\ell}{T}\right)^2 = 0.167 \Delta P (L_F/T)^2 \quad (\text{C7})$$

K is a function used to calculate the irradiation-enhanced creep strain. Combining Eqs. (C5), (C6), and (C7), and multiplying by 2 (because f of Eq. (C5) applies to only one side of a duct) gives Eq. (C2) where  $\chi$  is the maximum increase in distance across flats due to rounding from irradiation creep resulting from internal pressure, assuming that the stress, Eq. (C7), remains constant with time.

To take into account stress relaxation due to strain,  $\sigma$  (and thus  $\chi$ ) is multiplied by a factor which is equal to unity when the strain is zero, and equal to 0.5 when f is large enough to indicate the hex duct has become circular. (When a hex duct becomes circular, the bending stress  $\sigma$  becomes zero; therefore, the time-averaged value of  $\sigma$  while a hex duct is becoming circular is about one-half of the zero-strain value.)

The perimeter of a hex duct equals  $6 L_F/\sqrt{3}$  and the perimeter of a circular duct equals  $\pi D$ . Because both perimeters are equivalent,  $L_F/D = 0.909$ . That is, when  $2f = 0.1 L_F$ , the duct has become circular. Therefore, the aforementioned factor is about

$$\text{Factor} = 1 - \frac{0.5 (2f)}{0.1 L_F}$$

Consequently,

$$\begin{aligned} 2f &= \chi [1 - 5 (2F)/L_F] \\ &= L_F \chi / (L_F + 5\chi) \end{aligned}$$

which is the first term in Eq. (C1).

(2) Duct Swelling Dilation. The second term in Eq. (C1) merely states that the across-flat dimension of the duct increases by one-third of the fractional volumetric swelling.

(3) Handling and Bowing Allowance. The third term in Eq. (C2) comes from

$$0.030 (L_F + 2T)/2.29$$

which is based on the fact that the EBR-II ducts, with  $(L_F + 2T)$  equal to 2.29 in., were provided with a 0.030 in. gap for handling. It is assumed that this gap should be proportional to  $(L_F + 2T)$ , particularly when permanently and temporarily bowed ducts are considered.

Table C.1Nomenclature

<u>Symbols</u>	<u>Description</u>	<u>Typical Units</u>
c	Distance from surface to neutral axis	in.
D	Diameter	in.
E	Young's modulus	lb-in. <sup>-2</sup>
$\bar{E}$	Mean neutron energy	Me
f	Max. transverse deflection of one hex duct flat	in.
g	Transverse gap between adjacent ducts	in.
I	Moment of inertia	in. <sup>4</sup>
L <sub>F</sub>	Inside distance across duct flats	in.
ℓ	Length of beam (Inside width of duct flat)	in.
M	Bending moment	lb-in.
P	Pressure	lb-in. <sup>-2</sup>
T	Duct wall thickness	in.
V	Volume	in. <sup>3</sup>
W <sub>art</sub>	Unit load (artificial)	lb-in. <sup>-1</sup>
χ	Eq. (G.3)	
ε	Strain	in.-in. <sup>-1</sup>
σ	Stress	lb-in. <sup>-2</sup>

## References

1. G. W. Cunningham, "Advanced Breeder Fuel Development Program 1975-1985," Trans. Am. Nucl. Soc. 19, 83 (1974).
2. H. Mikailoff, J. Ravier, R. Lallement, "Review of the French Carbide Irradiation Program," Trans. Am. Nucl. Soc. 19, 84 (1974).
3. G. Karsten, "The Current SNR Advanced Fuels and Materials Program," Trans. Am. Nucl. Soc. 19, 84-85 (1974).
4. "Updated (1970) Cost-Benefit Analysis of the U.S. Breeder Reactor Program," WASH-1184 (January 1972).
5. Personal communication, M. King (ANL) to W. P. Barthold (ANL), February 17, 1976.
6. E. H. Novendstern, "Turbulent Flow Pressure Drop Model for Fuel Rod Assemblies Utilizing a Helical Wire-Wrap Spacer System," Nuclear Engineering and Design 22, (1972).
7. Letter, A. Boltax to W. P. Barthold, "Grid Design Data for Advanced Fuels System Design Studies," dated April 25, 1975.
8. A. B. G. Washington, "Preferred Values for the Thermal Conductivity of Sintered Ceramic Fuel for Fast Reactor Use," TRG-Report-2236, (September 1973).
9. Personal communication, R. McCandless (GE) to W. P. Barthold (ANL), April 1976.
10. Personal communication, J. Barner (LASL) to W. P. Barthold (ANL), February 1975.
11. M. C. Billone et al., "UNCLE - A Computer Code to Predict the Per-

- formance of Advanced Fuels in Breeder Reactors," Trans. Am. Nucl. Soc. 19, (1974).
12. Based on preliminary EBR-II data (1974).
  13. J. J. Laidler, "Development of Stress Free Swelling Design Equation," HEDL-TC November 1973, also "Alloy Properties Databook, Rev. 1," TC-293 (1975).
  14. W. P. Barthold, "Constrained Nuclear Design," Proc. ANS Meeting, Advanced Reactors; Physics Design, Economics (Sept. 8-11, 1974).
  15. Personal communication, R. McCandless (GE) to W. P. Barthold (ANL), April 1976.
  16. T. W. Latimer, J. O. Barner, J. F. Kerrisk, J. L. Green, "Post-irradiation Results and Evaluation of Helium-Bonded Uranium-Plutonium Carbide Fuel Elements Irradiated in EBR-II, Interim Report," LA-6249-MS (April 1976).
  17. Personal communication, Y. I. Chang (ANL) to W. P. Barthold (ANL), February 1976.
  18. T. W. Latimer, D. S. Bost, J. F. Kerrisk, J. O. Barner, J. L. Green, "Postirradiation Results and Evaluation of Sodium-Bonded Uranium-Plutonium Carbide Fuel Elements Irradiated in EBR-II, Interim Report," LA-6077-MS (December 1975).
  19. Personal communication, J. Beitel (ANL) to W. P. Barthold (ANL), June 1975.
  20. B. J. Toppel, "The New Multigroup Cross Section Code MC<sup>2</sup>-2," Proceedings of Conference on New Developments in Reactor Mathematics and Applications, CONF-710307 (1971).

21. P. A. Pizzica, D. A. Meneley, "SYNBURN - A Fast Reactor Fuel Cycle Program," ANL-76-14 (January 1976).
22. W. L. Woodruff et al., "The ARC System Standard Patterns and Catalogued Procedures," ANL-7712 (December 1971).
23. D. A. Meneley et al., "MACH-1, A One-Dimensional Diffusion-Theory Package," ANL-7223 (June 1966), pp. 32.
24. T. A. Daly et al., "The ARC System Two-Dimensional Diffusion Theory Capability, DARC2D," ANL-7716 (1972).
25. D. R. Ferguson, K. L. Derstine, R. C. Borg, T. A. Daly, "Optimal Iteration Strategies for Fast Reactor Finite Difference Diffusion Theory Codes," Trans. Am. Nucl. Soc. 22, 245 (1975).
26. D. R. Vondy et al., "VENTURE: A Code Block for Solving Multigroup Neutronics Problems Applying the Finite-Difference Diffusion-Theory Approximation to Neutron Transport," ORNL-5062 (1975).
27. C. H. Adams, "SYN3D - A Single-Channel, Spatial Flux Synthesis Code for Diffusion Theory Calculations," FRA-TM-81 (January 30, 1976).
28. See Ref. 22, pp. 158.
29. See Ref. 22, pp. 185.
30. A. E. Olson et al., "A User's Manual for the Reactor Burnup System REBUS-2," FRA-TM-62 (1972).
31. W. W. Little, Jr., R. W. Hardie, "2DB User's Manual," BNWL-831 (1968).
32. Reactor Development Program Progress Report,
  - a) July - August 1975, ANL-RDP-42, pp. 6.28,
  - b) October 1975, ANL-RDP-44, pp. 6.10.
33. W. W. Engle, Jr., "User's Manual for ANISN, A One-Dimensional Discrete Ordinates Transport Code with Anisotropic Scattering,"

- Computing Technology Center, Union Carbide Nuclear Division, K-1693, (1967).
34. W. A. Rhoades, F. R. Mynatt, "The DOT III Two-Dimensional Discrete Ordinates Transport Code," ORNL-TM-4280, September 1973.
  35. K. D. Lathrop, F. W. Brinkley, "TWOTRAN-II: An Interfaced, Exportable Version of the TWOTRAN Code for Two-Dimensional Transport," LA-4848-MS (July 1973).
  36. C. P. Tzanos, "A Computer Program for Reactivity and Power Shape Control," Trans. Am. Nucl. Soc. 23, 274-275 (1976).
  37. R. O. Gumprecht, "Mathematical Basis of Computer Code RIBD," DUN-4136 (1968).
  38. M. Bell, "ORIGEN - The ORNL Isotope Generation and Depletion Code," ORNL-4628 (1973).
  39. J. Beitel, "A User's Manual for the Core Temperature Calculation Package HEXFLO," in preparation.
  40. E. U. Khan, "A Porous Body Model for Predicting Temperature Distributions in Wire Wrapped Fuel and Blanket Assemblies for a Liquid Metal Fast Breeder Reactor," M.I.T. Thesis, 1974.
  41. R. C. Noyes, R. Pauze, "THESAC - A Thermal and Hydraulic Analysis Code for Sodium Fast Reactor Survey Calculation," LMFBR Technical Note 4, Combustion Engineering.
  42. F. E. Dunn et al., "The SAS-3A LMFBR Accident Analysis Computer Code," ANL/RAS 75-17, April 1975.
  43. B. R. Ferguson, T. A. Daly, E. L. Fuller, "Improvement and Calculation with the Two-Dimensional Space-Time Kinetics Code FX2," Ann

- Arbor, CONF-730414, Vol. 2 (1973).
44. R. W. Hardie, W. E. Black, W. W. Little, "ALPS, A Linear Programming System for Forecasting Optimum Power Growth Patterns," HEDL-TME-72-31 (April 1972).
  45. G. A. McLennan, "NUBOW - A FORTRAN IV Program for the Static Elastic Analysis of Bowed Reactor Cores," ANL-8068, April 1974.
  46. W. T. Sha, R. C. Schmitt, "THI3D - A Computer Program for Steady-State Thermal-Hydraulic Multi-Channel Analysis," ANL-8112.
  47. D. S. Rowe, "COBRA IIIC: A Digital Computer Program for Steady State and Transient Thermal-Hydraulic Analysis of Rod Bundle Nuclear Fuel Elements," BNWL-1695.
  48. P. J. Fulford, J. N. Fox, T. R. Yackle, "CORTAC - A Core Restraint Transient Analysis Code: Preliminary User's Manual," ANL-CT-76-10 (July 1975).
  49. G. V. Neill, R. J. McCandless, "Description of COROPT Program," Internal GE-Test Breeder Reactor Department Memo, dated May 23, 1975.
  50. Personal communication, T. R. Bump (ANL) to W. P. Barthold (ANL), November 1974.
  51. I. Charak, T. R. Bump, B. K. Cha, "The Effect of Coolant Temperatures on Estimates of Fast Reactor Interassembly Spacing," Trans. Am. Nucl. Soc. 21, 382-383 (1975).
  52. W. P. Barthold, J. Beitel, Y. I. Chang, M. King, Y. Orechwa, T. Bump, B. K. Cha, I. Charak, F. Tebo, "Breeding Performance and Pin Diameter Optimization for Mixed Carbide and Nitride Fuels in 5000 MWt LMFBRs," January 1975 (Draft).